Research Article

Mohammed T. Hayajneh*, Faris M. AL-Oqla, and Mu'ayyad M. Al-Shrida

Hybrid green organic/inorganic filler polypropylene composites: Morphological study and mechanical performance investigations

https://doi.org/10.1515/epoly-2021-0074
received July 01, 2021; accepted August 17, 2021

Abstract: In this study, the morphological and mechanical performances of hybrid green organic and inorganic filler composites were investigated. Various hybrid reinforcements using natural waste fillers including lemon leaves and eggshells were utilized for the study. The tensile strength, tensile modulus, elongation to break, flexural strength, and flexural modulus were investigated for the composites with polypropylene matrix. The results revealed that eggshells composites had the best values for both tensile and flexural tests while lemon leaves composites had the lowest values. However, the hybrid filler (lemon leaves-eggshells) had intermediate values. The poor properties of lemon leaves were attributed to the agglomeration and weak bonding presented by the morphological analysis of the hybrid composites.

Keywords: hybrid composites, natural fibers, eggshell, polypropylene, mechanical performance

1 Introduction

In recent decades, synthetic polymers have become a strong competitor to metals in different industries, ranging from infrastructure to aerospace applications due to its lightness and corrosion resistance (1). Despite these properties, they had a negative environmental impact as the annual waste of plastics was estimated to exceed 300 million tons in 2015. This produces a vast amount of CO_2 and other poisonous elements during degradation (2,3). Therefore, researchers around the world have been turning toward bio-polymeric composites (bio-filler reinforced synthetic polymer matrix or bio/synthetic filler reinforced biopolymer matrix) to reduce the harmful effects of synthetic polymer on the environment. Among bio-polymeric composites, natural fabric composites have aroused great interest due to their internal natural fibers that exhibit good properties such as availability, lightness, low cost, and good mechanical, thermal, and electrical properties along with the most important quality of biodegradability (4–7).

Diverse types of single and hybrid natural fibers like corn silk/*Hibiscus cannabinus* (8), waste tea leaves (9), olive leaves (10,11), Jordanian natural fiber species (12,13), sweet lime and lemon (14), and rice husk (15) have been fabricated with various polymer matrices. In addition to the organic natural fibers, inorganic fillers like glass fiber, carbon fiber, calcium carbonate, fly ash, etc., can also be used to reinforce polypropylene (PP) (16). Among inorganic fillers, eggshells (Es) can be a candidate to reinforce PP due to its characteristics like thermal stability, low price, availability, and user friendliness (17,18).

The advantages of PP, such as thermal stability, lightweight, relative low cost of processing, recyclability, and resistance to harsh conditions (19), make it one of the most common candidates for use as a matrix. On the other hand, PP suffers from low strength and modulus and low thermal conductivity (20). Consequently, engineers have been struggling to improve the mechanical, thermal, and tribological properties of the PP matrix by incorporating different organic and/or inorganic fillers (6,19,21,22). However, the effects of hybrid organic–inorganic reinforcement on the mechanical and thermal properties of PP have not been fully explored. So, the current study is trying to predict the mechanical characteristics

* **Corresponding author: Mohammed T. Hayajneh,** Industrial Engineering Department, Faculty of Engineering, Jordan University of Science and Technology, Irbid, Jordan,
e-mail: hayajneh@just.edu.jo
Faris M. AL-Oqla: Department of Mechanical Engineering, Faculty of Engineering, The Hashemite University, Zarqa 13133, Jordan,
e-mail: Fmaloqla@hu.edu.jo
Mu'ayyad M. Al-Shrida: Industrial Engineering Department, Faculty of Engineering, Jordan University of Science and Technology, Irbid, Jordan, e-mail: mmalshrida15@eng.just.edu.jo
ORCID: Mohammed T. Hayajneh 0000-0001-8328-2071; Faris M. AL-Oqla 0000-0002-6724-8567; Mu'ayyad M. Al-Shrida 0000-0001-6064-9125

(modulus and strength) and demonstrate that such fillers would be thermally stable during the manufacturing process of embedding PP with hybrid organic–inorganic reinforcement containing different percentages of lemon leaves fiber and Es reinforcement.

2 Materials and methods

2.1 Materials

In this study, virgin PP was used as matrix in the form of granules. It was provided from SABIC-Saudi Arabia (density = 0.9 g·cm^{-3}, thermal conductivity = 0.26 W·(m·K)$^{-1}$.

The organic filler lemon leaves were used as the first filler in the PP matrix. No treatments were conducted on the lemon leaves to enhance its properties before utilizing it as a raw material in such composite materials. They were taken as it is from Jordanian lemon trees. The preparation of lemon leaves passed through many steps. The first step was the collection and cutting of the leaves from a local tree, as seen in Figure 1a. Second, the fibers were chopped into small pieces by scissors as shown in Figure 1b. Third, the leaves were placed into a blender converting them into lemon (L) leaves fiber containing midrib, lamina, and vein as revealed in Figure 1c and d, and eventually, a random sample of 35 midribs and 35 laminas were selected to calculate the average and standard deviation of their lengths as shown in Figure 1e and f. The mean and standard deviation of the midribs were 21 ± 13.4 mm while the mean and standard deviation of the laminas were approximately 6 ± 4.5 mm. The density of the entire L is 0.78 g·cm^{-3} as calculated from the Archimedes rule. The surface morphology of L fiber was investigated by using a scanning electron microscope (SEM) in Section 3.3.

Es, an inorganic filler, were used as the second filler without any treatments in the PP matrix. The green waste Es is considered as an inorganic filler because 95% of it is composed of calcium carbonate (23). The shells were gathered from various bakeries. Then, they were sprayed with water to clean the remnants of yolks and albumen. After that, the shells were dried in the sun and broken into small flakes. Finally, a random small pile of 35 flakes of the shells was taken to find the close length of the shells' fragments. The mean and standard deviation were 3.6 and 1.5 mm, respectively. The density was measured in our previous studies (17,18) and it was 2.5 g·cm^{-3}. Figure 2

Figure 1: Preparation of the lemon fiber: (a) collecting lemon leaves, (b) chopping by scissors, (c) chopping by blender blades, (d) pile of midribs and laminas of lemon leaves, (e) measuring the approximate length of midribs, and (f) laminas by ruler.

Figure 2: The stages of shells' preparation including (a) gathering, (b) flaking, and (c) measuring the length of the shells by ruler.

displays the various stages of preparing the shells. The topography of Es is presented in Section 3.3.

2.2 Composite processing

Mono composite and hybrid composite were prepared using the three weight percentages of the fillers (5, 10, and 20 wt%) of L, Es, and H (50 wt% of L and 50 wt% of Es). First, the compound of the matrix and the filler was mixed manually. Then, the compound was placed into a locally manufactured single-screw extruder. Finally, the extruded mixtures were compressed by four tones at room temperature in a rectangular mold with the dimensions of 100 mm × 70 mm × 5 mm. The output zone temperature of the extruder was in the range of 200–220°C. The weight percentages and the codes of the composites are presented in Table 1.

2.3 Tensile test

The tensile properties like tensile strength, modulus of elasticity, and elongation at break were determined according to the ASTM D3039-3039M at a crosshead speed of 2 mm·min^{-1}. The test was performed in a uniaxial direction on a universal testing machine (UTM; model WDW-20). The dimensions of the samples were 80 mm × 20 mm × 5 mm with a gauge length of 50 mm.

Table 1: The codes and weight percentages of the composites

Sample code	L (wt%)	Es (wt%)	PP (wt%)
PP	0	0	100
5 L–PP	5	0	95
10 L–PP	10	0	90
20 L–PP	20	0	80
5 Es–PP	0	5	95
10 Es–PP	0	10	90
20 Es–PP	0	20	80
5 H–PP	2.5	2.5	95
10 H–PP	5	5	90
20 H–PP	10	10	80

2.4 Flexural test

A three-point bending test was used to determine the flexural strength, which represents the highest flexural stress on the stress–strain curve, and the flexural modulus (E_f) which can be calculated from the ratio of flexural stress (σ_f) to flexural strain (ε_f) within the elastic region. Flexural stress, flexural strain, and flexural modulus were calculated according to the Eqs. 1–3, respectively. The test was performed on a UTM (model WDW-20) according to ASTM D790 at room temperature with a crosshead speed of 2 mm·min^{-1}. Rectangular specimens were cut from the original sheets with dimensions of 100 mm × 10 mm × 5 mm.

$$\sigma_f = \frac{3FL}{2WT^2} \tag{1}$$

where σ_f and F represent the flexural stress (in MPa) and the applied force (in N), while W, T, and L represent the width (in mm), the thickness (in mm), and support span (in mm), respectively.

$$\varepsilon_f = \frac{6DT}{L^2} \tag{2}$$

where ε_f is the flexural strain and D is the maximum deflection at the center of the specimen in mm. T and L are the thickness and the support span in mm.

$$E_f = \frac{\Delta\sigma_f}{\Delta\varepsilon_f} \tag{3}$$

2.5 Scanning electron microscope characterization

A SEM (Quanta™ 450 FEG SEM) was used to investigate the distribution of fiber in the matrix, pull-out phenomenon, and the bonding at the matrix–fiber interface after the tensile test. Also, the morphology of the raw fibers was characterized by SEM. All samples were sputtered with a gold layer of 18 nm prior to SEM examination to avoid electrostatic charging.

3 Results and discussion

3.1 Tensile test

3.1.1 Tensile modulus

The tensile modulus of elasticity for mono composites (L–PP or Es–PP) and hybrid composites (H–PP) are presented in Figure 3. It is evident from the figure that L filler improves the modulus value of PP at 5 L wt%. At 10 L wt%, unlike 10 Es and 10 H wt%, the modulus value dropped significantly to reach the lowest value among all samples. At 20 L wt% the tensile modulus increased again to reach the neat value. This trend may be attributed to stress concentration. The addition of an insufficient amount of filler leads to stress concentration, which speeds up the failure process in the composite. The inadequate amount does not allow the reinforcement to do its main function, that is, resisting the external load. At 5 L wt%, the stress concentration is very small, and the fibers partially do their role which leads to initial improvement. However, at 10 L wt%, the stress concentration increased, leading to lower modulus. At 20 wt%, it sounds that the L fibers begin to withstand the external forces which may explain the improvement of modulus. Similar results were obtained by Zanini et al. (24) for palm fiber–PP composites.

According to Es–PP composites, a different trend is observed. The tensile modulus at 5 Es wt% increased by 15%, whereas at 10 Es wt% the tensile modulus touches the highest value to reach an improvement of 21%. Nevertheless, at 20 Es wt%, the modulus diminished again, but it is still higher than the tensile modulus of neat PP. The improvement of moduli at 5 and 10 wt% of Es refers to the nature of stiff bio-filler Es where the stiffness property indicates the modulus. On the other hand, the decline in tensile modulus at 20 Es wt% may refer to the agglomerates that are presented later in Section 3.3.2. A similar trend was reported by Ghabeer et al. (25).

The behavior of H-composites differs from L and Es composites, where the tensile modulus decreased gradually while increasing the weight percentage of H filler. Despite this decline, the moduli of H-composites exceeded PP modulus, and achieved the highest improvement of 19% at 5 H wt%.

The L composites achieved the lowest values when compared to Es and H composites. The cause behind this might be the poor bonding at the L–PP interface. Not only

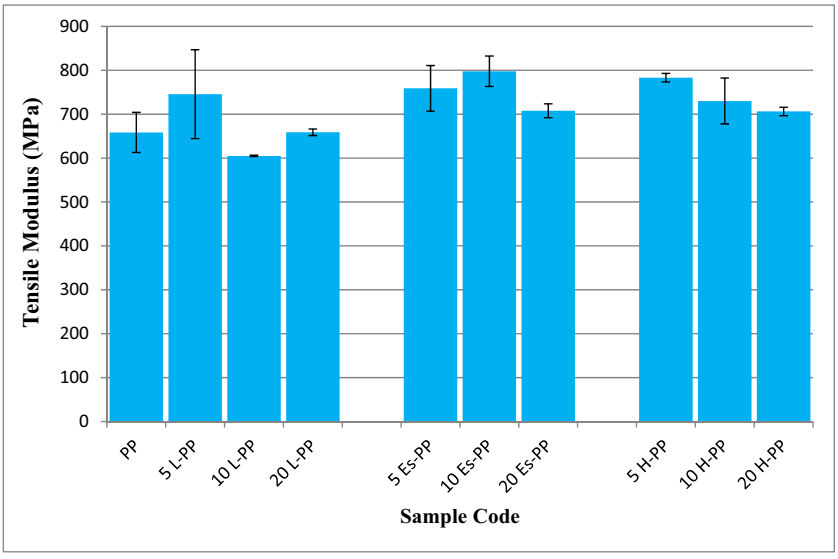

Figure 3: The tensile modulus values of mono and hybrid composites.

that, the agglomeration phenomenon due to poor mixing may contribute to the aforementioned result. This interpretation is presented by SEM in Section 3.3.

3.1.2 Tensile strength

Figure 4 displays the tensile strength for all composites (L–PP, Es–PP, and H–PP). It is conspicuous that all types of composites have lower tensile strength than neat PP. The group of L composites shows the same trend that is observed in tensile modulus but with lower values. The tensile strength diminished to reach the lowest value at 10 L wt% among all composites and again increased at 20 L wt%. The same interpretation that was used in tensile modulus for this trend may be valid here. In addition to that, the decrease in tensile strength in L–PP composites below the tensile strength of PP can be attributed to the weak adhesion between L fiber and PP matrix which facilitates the pull-out phenomenon leading to hastening the failure of the composite and therefore reducing the tensile value. On top of that, the agglomeration of L fiber prevents matrix–matrix contact and causes an internal weak mesh prompting faster failure. This is displayed

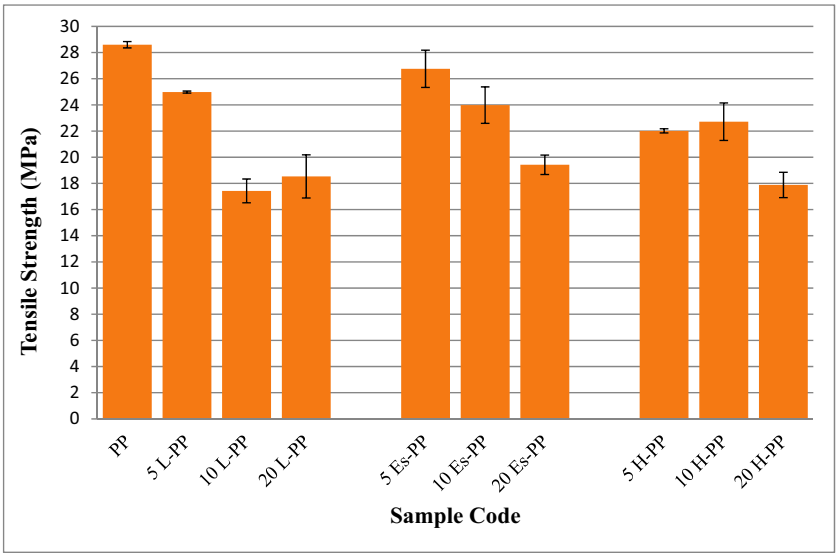

Figure 4: The tensile strength values of mono and hybrid composites.

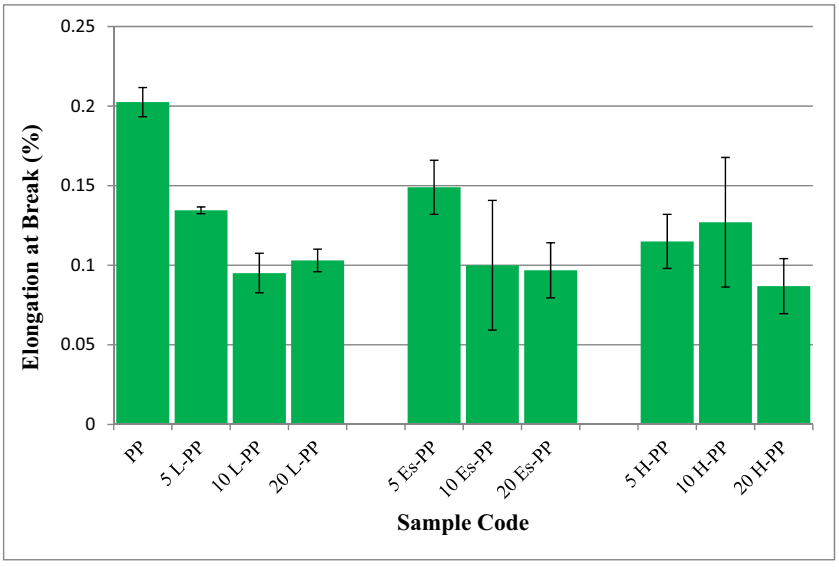

Figure 5: The elongation at break values for all composites.

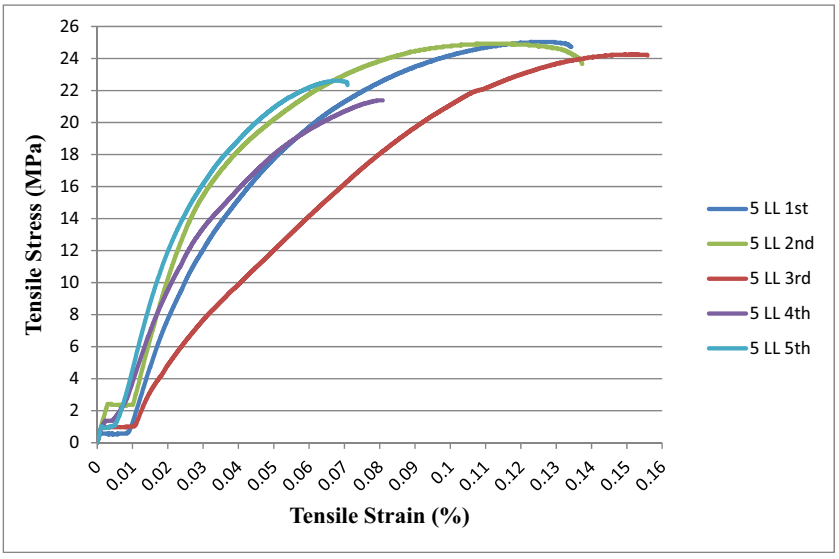

Figure 6: Stress–strain behavior of five replicates of five L–PP composite.

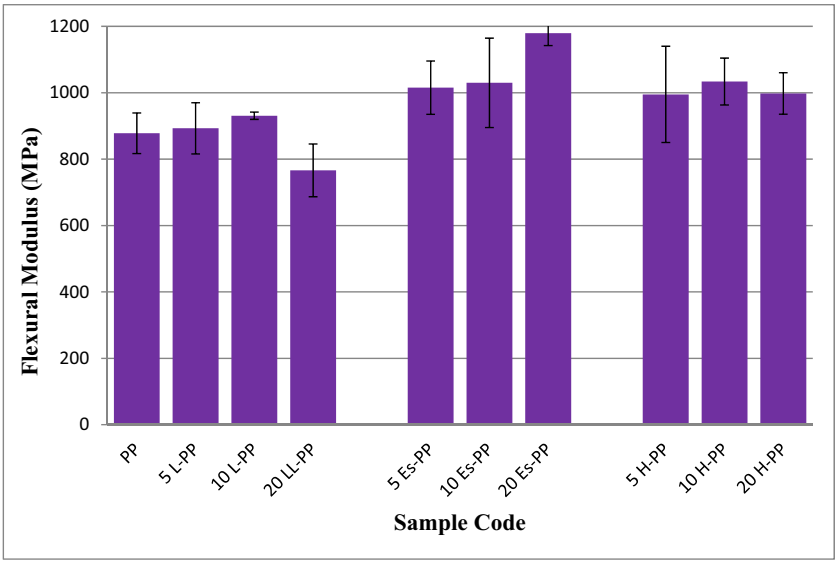

Figure 7: The flexural modulus values of mono and hybrid composites.

by SEM micrographs. Ghabeer et al. (25) recorded very similar observations.

Although the Es composites do not reach the tensile strength of neat PP, they get better results when compared to L composites. It is expected that Es reduce the tensile strength of PP because of the nature of stiff bio-ceramic Es. Also, better results may refer to lower agglomeration of Es in the PP matrix, since the density of Es is relatively high when compared to L and thus the lower volume of Es filler. Further, the relative improvement can be attributed to better adhesion between Es and PP as explained in Section 3.3.

The addition of hybrid filler (Es + L) also reduces the tensile strength of PP as shown in Figure 4. The 5 and 10 wt% of fillers give a very close tensile strength value that dropped significantly at 20 wt% due to agglomeration.

3.1.3 Elongation at break

It is evident from Figure 5 that the elongation at break for all composites diminished generally with the increasing weight percentage of fillers regardless of the type of filler.

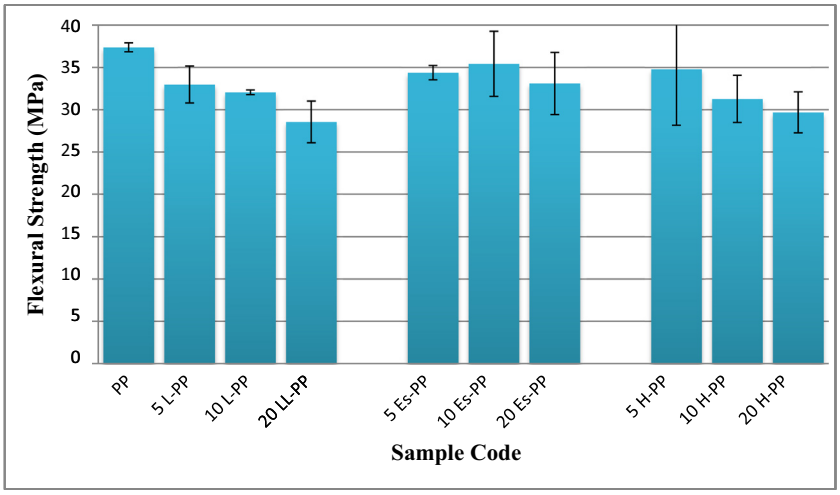

Figure 8: The flexural strength values of mono and hybrid composites.

Actually, such a trend is forecasted since the addition of fillers makes the matrix brittle. The trend of elongation at break matches the trend of tensile strength with different values. The elongation at break value of 0.2% for PP is also reported by Kumar et al. (26).

3.1.4 Stress–strain behavior

The tensile stress–strain behavior of the five replicates of five L–PP composites is depicted in Figure 6. It is demonstrated from the replicates in the figure that the variations of tensile strength are marginal where the standard deviation did not exceed 1.6 MPa. However, the variation within the tensile moduli and elongations at break is higher than that presented within the tensile strength. This variation is expected due to the random orientation of the fillers inside the matrix that may cause some fiber agglomeration leading to poor fiber distribution and lower adhesion with the matrix. Thus, several replicates were considered according to the standard tensile test, and the average values were considered. An irregular behavior at the birth of the curve is detected in all replicates. This may be associated with the sample slipping during the beginning of load applying.

3.2 Flexural test

The results of flexural modulus and flexural strength of L, Es, and H composites are depicted in Figures 7 and 8,

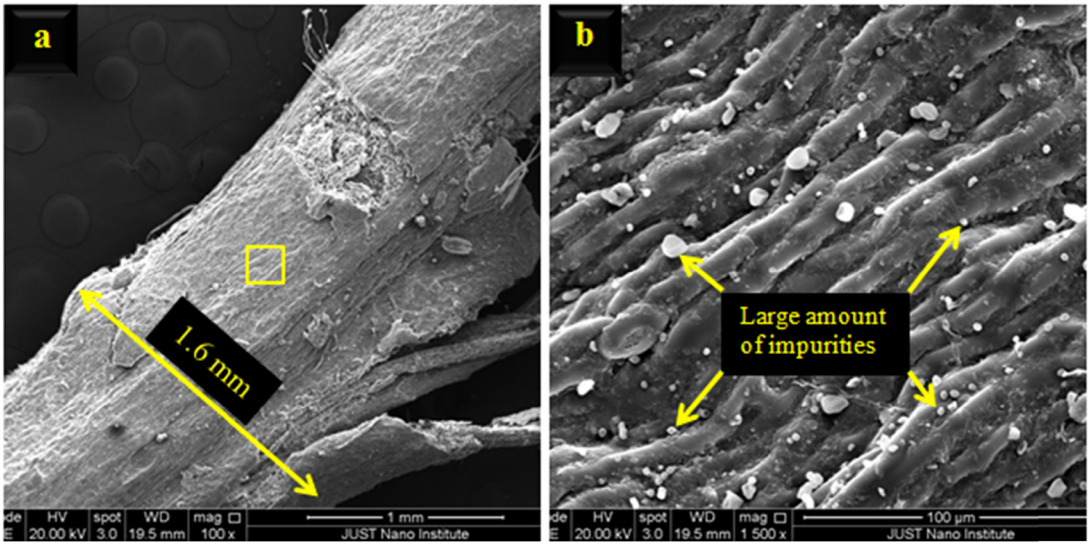

Figure 9: SEM micrograph of lemon leaf midrib: micrograph (b) is a magnification for the yellow square in micrograph (a).

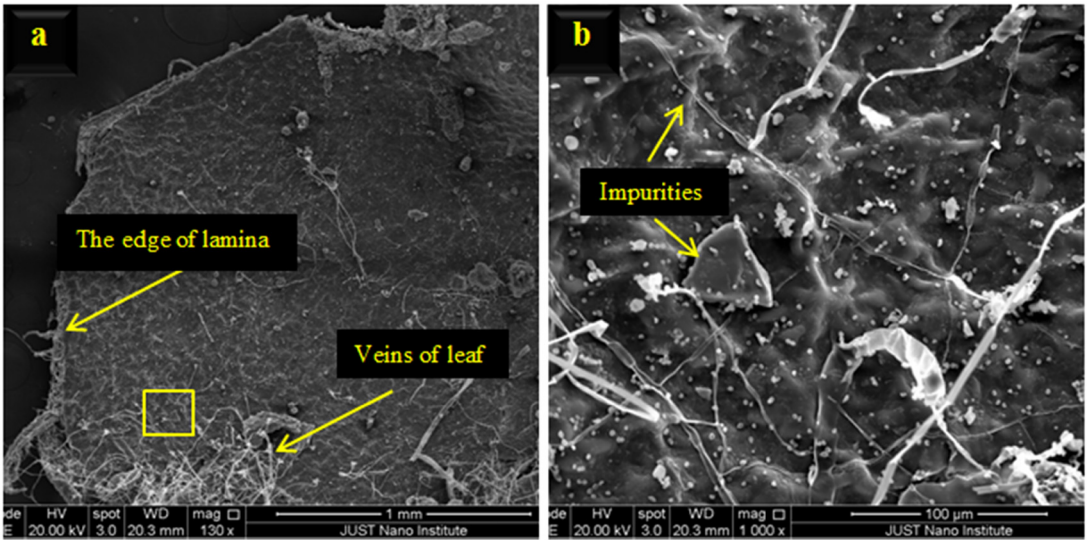

Figure 10: SEM micrograph of a small flake of lemon leaf (lamina and veins): micrograph (b) is a magnification for the yellow square in micrograph (a).

respectively. Figure 7 presents that all levels (5, 10, and 20 wt%) of reinforcements improved the flexural modulus regardless of the type of filler except at 20 L wt% which adversely affected the flexural modulus where it worsened the flexural modulus of neat PP. The improvement of flexural modulus may be attributed to the used stiff fillers, while the flexural modulus dropping at 20 L wt% may refer to the high fiber–fiber interactions due to the dispersion problem of natural L as presented in the SEM micrograph (Section 3.3.2). The decrease in the flexural modulus at high weight percentage was reported by Arib et al. (18) for the pineapple leaf–PP composite. Figure 7 also shows that all Es composites have the highest values of flexural modulus compared to L and H composites. The flexural modulus reaches the vertex at 20 Es wt% where it was improved by 34%.

In the case of L composites, the flexural moduli are generally lower than those in the Es composites. This may be due to numerous causes. First, the poor bonding at the L–PP interface. Second, the agglomeration of L fiber may occur due to the poor mixing condition and the higher cross-sectional areas of L which hinder the dispersion of L in the PP matrix (27). The aforementioned problems will be discussed in Section 3.3.2.

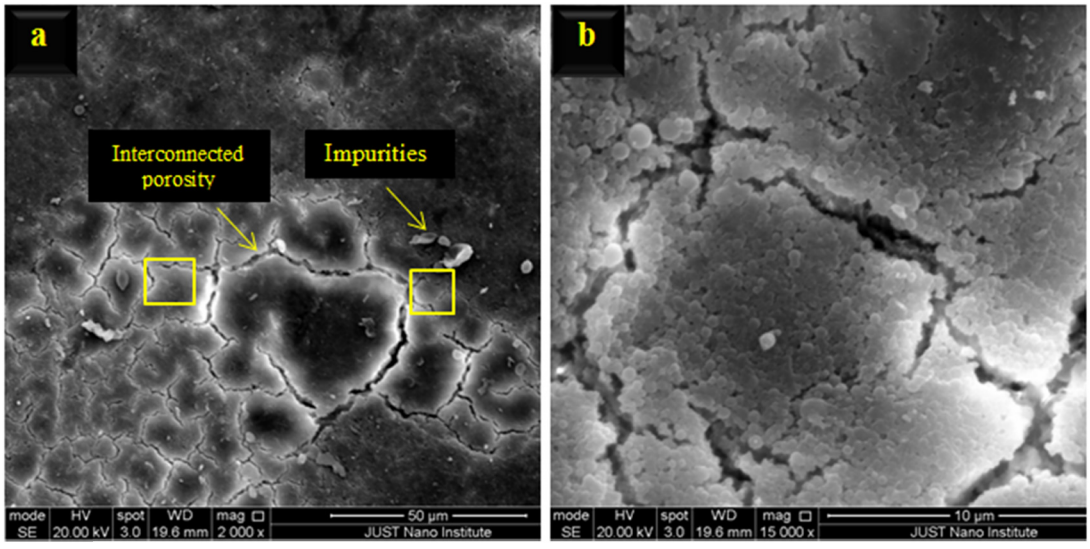

Figure 11: SEM micrograph of the outer surface of Es flake: micrograph (b) is a magnification for the yellow square in micrograph (a).

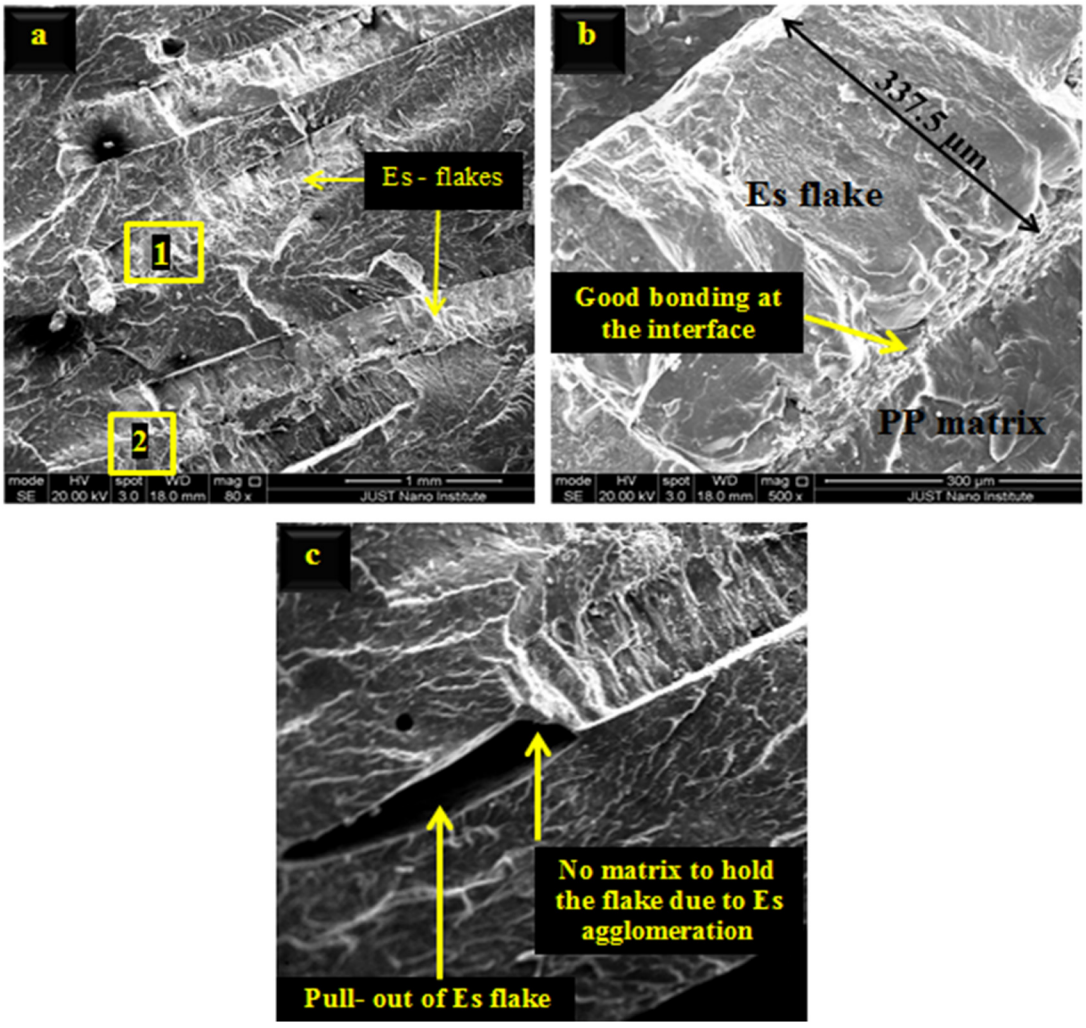

Figure 12: SEM micrograph of 20 Es–PP composite: micrograph (b) is a magnification for the first square in micrograph (a) and micrograph (c) is a magnification for the second square in micrograph (a).

According to Figure 8, it can be observed that the flexural strength of Es composites has the highest values among the other fillers (L and H) despite the fact that they did not touch the strength of neat PP. At 20 wt% of the three types of fillers, the composites get the lowest values. This might be due to the reason discussed before. Kumar et al. (26) recorded an increase in flexural modulus from 1,300 MPa for PP to 1,426 MPa for PP with 20 wt% of Es.

For the composites with H filler, they get approximately intermediate values between Es and L composites for flexural and tensile strength. Actually, this will be rational if the rule of mixture is applied. Although the results of flexural and tensile tests are similar, the flexural test gave better results when compared to the tensile test because in the flexural test only the central part of the sample is affected by load, while in the tensile test the whole sample is exposed to load. Therefore, if the void is not in the center, its contribution will be insignificant in the fracture (7).

3.3 Morphological analysis

3.3.1 The surface morphology of fiber

The morphology of the midrib and lamina of the lemon leaf was investigated by SEM as shown in Figures 9 and 10, respectively. It could be observed from Figures 9 and 10 that there is a significant amount of impurities on the surface of the midrib (Figure 9) and lamina (Figure 10) fiber because no attempt was made to treat or even clean the fiber. Furthermore, no pits are observed on the surface of the fiber, midrib, and lamina, which indicate the

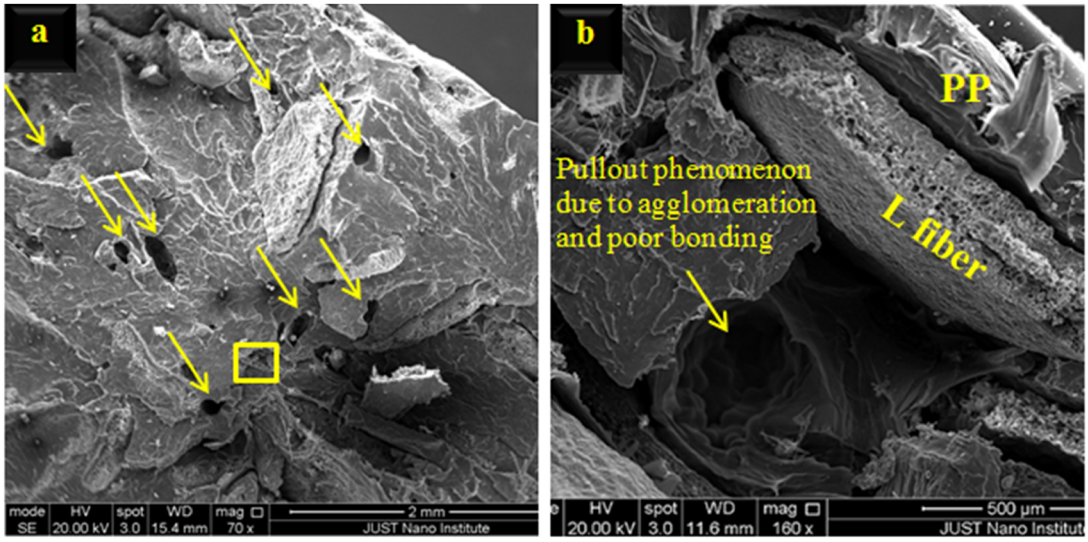

Figure 13: SEM micrograph of 20 Es–PP composite: micrograph (b) is a magnification for the yellow square in micrograph (a). Yellow arrows in micrograph (a) indicate pull-out.

existence of the waxy layer and lignin (28).The waxy layer, impurities, and smooth surface may have a role in the weak bonding with PP which results in poorer mechanical properties compared to Es filler. Moreover, it can be found that the midrib and lamina have different topography which may lead to different bonding behavior.

Figure 11 presents the morphology of the outer surface of Es flake. It can be observed that the impurities on the surface of the shell are actually lower than that in L fiber. Also, the interconnected porosity shown in Figure 11 refers to the nature of porous Es. The lower impurities and the rougher surface of Es may have a positive impact on bonding behavior.

3.3.2 The surface morphology of fractured composites

The microstructure of fractured composites (20 Es–PP and 20 L–PP) after the tensile test was investigated by SEM, is shown in Figures 12 and 13. It can be seen from Figure 12a that the distribution of Es flakes though PP matrix is almost good, and the agglomerates found in the Es composite are lower than that in L composite as seen in Figure 13b. The agglomeration facilitates the pull-out phenomenon because there is no matrix to hold the fiber (Figure 12c) speeding up the failure process which in turn interprets the significant reduction in tensile strength and modulus at 20 wt%. Furthermore, Figure 12c shows good bonding at the interface between PP and Es. Figure 12b also shows a transverse cross-section of Es flake. So, the thickness used in the flake can be measured.

Figure 13b clears the poor bonding between L fiber and PP matrix. However, Figure 13a shows a large number of pull-outs of L fiber which might make the tensile and flexural values of 20 L–PP composites lower than the tensile and flexural values of 20 Es–PP. If Figure 13a is compared with Figure 12a, it will be easy to note that the number of pull-outs in L composite is much higher than that in the Es composite.

4 Conclusion

Green Es and hybrid fillers had positive effects on the flexural and tensile modulus of neat PP regardless of weight percentages, but lemon filler worsened both flexural and tensile modulus at specific weight percentages. On the other hand, all fillers reduced the values of tensile strength and flexural strength of PP. In any case, the hybrid filler obtained in-between results compared to lemon and Es fillers. Moreover, it can be revealed that Es are better than lemon leaves in all mechanical properties at all percentages. Furthermore, it can be noted that 20 wt% of H and Es filler reduced the tensile and flexural strength. It may refer to the agglomeration of fiber in the PP matrix as shown in SEM images.

Funding information: This work was supported by a grant from the Deanship of Scientific Research at the Jordan University of Science and Technology (JUST) with Grant no. 448/2019.

Author contributions: The manuscript was written with the contributions of all authors. All authors have given approval to the final version of the manuscript.

Conflict of interest: Authors state no conflict of interest.

References

(1) Rodriguez V, Sukumaran J, Schlarb AK, Baets PDe. Reciprocating sliding wear behaviour of PEEK-based hybrid composites. Wear. 2016;362–363:161–9. doi: 10.1016/j.wear.2016.05.024.

(2) Karan H, Funk C, Grabert M, Oey M, Hankamer B. Green bioplastics as part of a circular bioeconomy. Trends Plant Sci. 2019;24(3):237–49. doi: 10.1016/j.tplants.2018.11.010.

(3) Zhang S, Zhang Z, Kang D, Bang D, Kim J. Preparation and characterization of thermoplastic elastomers (TPEs) based on waste polypropylene and waste ground rubber tire powder. e-Polymers. 2008;8(1):160. doi: 10.1515/epoly.2008.8.1.1839.

(4) AL-Oqla FM. Investigating the mechanical performance deterioration of mediterranean cellulosic cypress and pine/polyethylene composites. Cellulose. 2017;24(6):2523–30. doi: 10.1007/s10570-017-1280-3.

(5) AL-Oqla FM, Sapuan SM. Natural fiber reinforced polymer composites in industrial applications: feasibility of date palm fibers for sustainable automotive industry. J Clean Prod. 2014;66:347–54. doi: 10.1016/j.jclepro.2013.10.050.

(6) AL-Oqla FM, Hayajneh MT, Fares O. Investigating the mechanical thermal and polymer interfacial characteristics of Jordanian lignocellulosic fibers to demonstrate their capabilities for sustainable green materials. J Clean Prod. 2019;241:118256. doi: 10.1016/j.jclepro.2019.118256.

(7) Guna V, Ilangovan M, Hassan Rather M, Giridharan BV, Prajwal B, Vamshi Krishna K, et al. Groundnut shell/rice husk agro-waste reinforced polypropylene hybrid biocomposites. J Build Eng. 2020;27:100991. doi: 10.1016/j.jobe.2019.100991.

(8) Pandey J, Kim C, Chu W, Lee C, Jang D, Ahn S. Evaluation of morphological architecture of cellulose chains in grass during conversion from macro to nano dimensions. e-Polymers. 2009;9(1):102. doi: 10.1515/epoly.2009.9.1.1221.

(9) AL-Oqla FM, El-Shekeil YA. Investigating and predicting the performance deteriorations and trends of polyurethane biocomposites for more realistic sustainable design possibilities. J Clean Prod. 2019;222:865–70. doi: 10.1016/j.jclepro.2019.03.042.

(10) AL-Oqla FM. Flexural characteristics and impact rupture stress investigations of sustainable green olive leaves bio-composite materials. J Polym Environ. 2021;29:892–9. doi: 10.1007/s10924-020-01889-3.

(11) Aljnaid M, Banat R. Effect of coupling agents on the olive pomace-filled polypropylene composite. e-Polymers. 2021;21(1):377–90. doi: 10.1515/epoly-2021-0038.

(12) AL-Oqla FM, Hayajneh MT, Aldhirat A. Tribological and mechanical fracture performance of Mediterranean lignocellulosic fiber reinforced polypropylene composites. Polym Compos. 2021;1:1–13. doi: 10.1002/pc.26241.

(13) Hayajneh MT, AL-Oqla FM, Aldhirat A. Physical and mechanical inherent characteristic investigations of various Jordanian natural fiber species to reveal their potential for green biomaterials. J Nat Fibers. 2021;1:1–14. doi: 10.1080/15440478.2021.1944432.

(14) Patil AY, Umbrajkar Hrishikesh N, Basavaraj GD, Chalageri Gireesha R, Kodancha Krishnaraja G. Influence of biodegradable natural fiber embedded in polymer matrix. Mater Today: Proc. 2018;5(2):7532–40. doi: 10.1016/j.matpr.2017.11.425.

(15) Aridi NA, Sapuan SM, Zainudin ES, AL-Oqla FM. Mechanical and morphological properties of injection-molded rice husk polypropylene composites. Int J Polym Anal Charact. 2016;21(4):305–13. doi: 10.1080/1023666x.2016.1148316.

(16) Min Y, Huang R, He C, Wu Q, Zhao X. Hybrid composites from wheat straw, inorganic filler, and recycled polypropylene: morphology and mechanical and thermal expansion performance. Int J Polym Sci. 2016;2016:1–12. doi: 10.1155/2016/2520670.

(17) Almomani MA, Hayajneh MT, Al-Shrida MM. Investigation of mechanical and tribological properties of hybrid green eggshells and graphite-reinforced aluminum composites. J Braz Soc Mech Sci Eng. 2020;42(1):1–3. doi: 10.1007/s40430-019-2130z.

(18) Hayajneh MT, Almomani MA, Al-Shrida MM. Effects of waste eggshells addition on microstructures, mechanical, and tribological properties of green metal matrix composite. Sci Eng Compos Mater. 2019;26(1):423–34. doi: 10.1515/secm-2019-0027.

(19) Agarwal J, Mohanty S, Nayak SK. Influence of cellulose nanocrystal/sisal fiber on the mechanical, thermal, and morphological performance of polypropylene hybrid composites. Polym Bull. 2021;78:1609–35. doi: 10.1007/s00289-020-03178-4.

(20) Kada D, Koubaa A, Tabak G, Migneault S, Garnier B, Boudenne A. Tensile properties, thermal conductivity, and thermal stability of short carbon fiber reinforced polypropylene composites. Polym Compos. 2016;39(S2):E664–70. doi: 10.1002/pc.24093.

(21) Arib RMN, Sapuan SM, Ahmad MM, Paridah MT, Zaman HM. Mechanical properties of pineapple leaf fibre reinforced polypropylene composites. Mater Des. 2006;27(5):391–6. doi: 10.1016/j.matdes.2004.11.009.

(22) AL-Oqla FM, Sapuan SM, Ishak MR, Nuraini AA. A decision-making model for selecting the most appropriate natural fiber – polypropylene-based composites for automotive applications. J Compos Mater. 2016;50(4):543–56. doi: 10.1177/0021998315577233.

(23) Onwubu S, Phumlane S, Singh S, Madikizela L, Ngombane Y. Characterization and in vitro evaluation of an acid resistant nanosized dental eggshell-titanium dioxide material. Adv Powder Technol. 2019;30(4):766–73. doi: 10.1016/j.apt.2019.01.005.

(24) Zanini N, Barbosa R, Souza A, Rosa D, Mulinari D. Revaluation of australian palm residues in polypropylene composites: statistical influence of fiber treatment. J Compos Mater. 2020;55(6):813–26. doi: 10.1177/0021998320960534.

(25) Ghabeer T, Dweiri R, Al-Khateeb S. Thermal and mechanical characterization of polypropylene/eggshell biocomposites.

J Reinf Plast Compos. 2013;32(6):402–9. doi: 10.1177/0731684412470015.
(26) Kumar R, Dhaliwal JS, Kapur GS. Mechanical properties of modified biofiller-polypropylene composites. Polym Compos. 2013;35(4):708–14. doi: 10.1002/pc.22714.
(27) Alzebdeh K, Nassar M, Arunachalam R. Effect of fabrication parameters on strength of natural fiber polypropylene composites: statistical assessment. Measurement. 2019;146:195–207. doi: 10.1016/j.measurement.2019.06.012.
(28) Jain J, Jain S, Sinha S. Characterization and thermal kinetic analysis of pineapple leaf fibers and their reinforcement in epoxy. J Elastomers Plast. 2019;51(3):224–43. doi: 10.1177/0095244318783024.